CMLS, Cell. Mol. Life Sci. 62 (2005) 1763–1771
1420-682X/05/151763-09
DOI 10.1007/s00018-005-5185-1

CMLS Cellular and Molecular Life Sciences

Research Article

Antiproliferative activity of olomoucine II, a novel 2,6,9-trisubstituted purine cyclin-dependent kinase inhibitor

V. Kryštof[a], I. W. McNae[b], M. D. Walkinshaw[b], P. M. Fischer[c], P. Müller[d], B. Vojtěšek[d], M. Orság[a], L. Havlíček[a] and M. Strnad[a,*]

[a] Laboratory of Growth Regulators, Faculty of Science, Palacký University & Institute of Experimental Botany AS CR, Šlechtitelů 11, 783 71 Olomouc (The Czech Republic) Fax: + 420 585 634 870, e-mail: strnad@prfholnt.upol.cz
[b] Structural Biochemistry Group, The University of Edinburgh, Michael Swann Building, King's Buildings, Edinburgh, EH9 3JR, Scotland (UK)
[c] Cyclacel Limited, James Lindsay Place, Dundee DD1 5JJ, Scotland (UK)
[d] Department of Experimental Oncology, Masaryk Memorial Cancer Institute, Žlutý kopec 7, 656 53 Brno, (The Czech Republic)

Received 3 May 2005; received after revision 26 May 2005; accepted 8 June 2005
Online First 7 July 2005

Abstract. The study describes the protein kinase selectivity profile, as well as the binding mode of olomoucine II in the catalytic cleft of CDK2, as determined from co-crystal analysis. Apart from the main cell cycle-regulating kinase CDK2, olomoucine II exerts specificity for CDK7 and CDK9, with important functions in the regulation of RNA transcription. *In vitro* anticancer activity of the inhibitor in a panel of tumor cell lines shows a wide potency range with a slight preference for cells harboring a wild-type p53 gene. Cell-based assays confirmed activation of p53 protein levels and events leading to accumulation of $p21^{WAF1}$. Additionally, in olomoucine II-treated cells, Mdm2 was found to form a complex with the ribosomal protein L11, which inhibits Mdm2 ubiquitin ligase function. We conclude that perturbations in RNA synthesis may lead to activation of p53 and that this contributes to the antiproliferative potency of cyclin-dependent kinase inhibitors.

Key words. Olomoucine II; roscovitine; cyclin-dependent kinase inhibitor; CDK9; transcription; p53 mutation.

Neoplastic transformation is a sequence of genomic alterations, e.g. gain-of-function mutations resulting in oncoprotein activation, and loss-of-function mutations leading to inactivation of tumor-suppressor gene products [1]. As a consequence of these mutations, the transformed cell acquires the ability to proliferate in the absence of extracellular growth signals. This forced proliferative state is tightly connected with elevated levels of the principal cell cycle regulators, i.e. the cyclin-dependent kinases (CDKs). Individual CDKs associate with their cyclin-activating partners which are cell cycle phase-specific proteins. The various CDK-cyclin complexes reach maximum activity during particular phases, i.e. CDK4/CDK6-cyclin D and CDK2-cyclin E during G1, CDK2/cyclin A in S phase, and CDK1/cyclin B at the G2/M boundary [1, 2]. Furthermore, at least CDK7, CDK8, and CDK9 participate in the phosphorylation of the C-terminal domain (CTD) of RNA polymerase II and thus regulate transcription [3]. Altered protein phosphorylation patterns in cancer cells have stimulated an extensive search for protein kinase inhibitors with potential applications in cancer therapy [4, 5].
The discovery of olomoucine, one of the earliest reported specific CDK inhibitors led to the development of exten-

* Corresponding author.

sive research on structure-activity relationships within the 2,6,9-trisubstituted purine compound class to which olomoucine belongs [6]. Structural modifications to olomoucine culminated in the discovery of even more potent and CDK-selective antiproliferative purine inhibitors, such as roscovitine, purvalanol A, and now olomoucine II [7–9]. A chirally and chemically defined and pure form of *R*-roscovitine (seliciclib, CYC202, Cyclacel) is currently in phase II clinical trials in patients with cancer [4, 10, 11]. In recent years, a large number of pharmacological CDK inhibitors other than trisubstituted purines, with a wide variety of cellular antiproliferative mechanisms, have also been reported [5, 12]. The antiproliferative activities of such compounds have variously been associated with inhibition of CDK1/cyclin B, CDK2/cyclin E, CDK2/cyclin A, and, to a lesser extent, with CDK4/cyclin D, all kinases involved directly in the regulation of the cell cycle, and also with inhibition of CDK7/cyclin H, which forms part of the CDK-activating (CAK) complex [2, 5].

The CDK inhibitors roscovitine and flavopiridol are known to induce nuclear accumulation of the tumor suppressor protein p53, as well as to trigger its transcriptional activity in human cancer cells [13–18]. Accumulated p53 in turn induces a host of downstream genes, including those encoding the endogenous CDK inhibitor $p21^{WAF1}$ which executes cell cycle arrest, and the p53-specific ubiquitin ligase Mdm2 which negatively affects p53 activity and stability. However, unlike p53 transcriptional activity, p53 protein levels do not apparently respond to elevated Mdm2 [17]. Moreover, high doses of CDK inhibitors reduce expression of Mdm2 and $p21^{WAF1}$ [17; unpublished observation] as a result of interference with global transcription and selective down-regulation of proteins with short half-life mRNAs [8, 16, 18]. This may again lead to stabilization of p53 by suppressing the expression of Mdm2. Elsewhere, the pan-CDK specific inhibitor flavopiridol has been found to display similar effects, exerting its activity via several mechanisms, including interaction with CDK9 [19]. Despite the evidence showing that roscovitine-meditated p53 stabilization is linked to interference with transcription through inhibition of the CDKs that regulate RNA synthesis, such as CDK7 and 9 [16, 18], the mechanism of p53 stabilization by CDK inhibitors has not been fully explained. For example, roscovitine can also inhibit rRNA synthesis, leading to nucleolar disruption [20, 21].

The enhanced *in vitro* anticancer activity of olomoucine II compared e.g. to the structurally related roscovitine [9] motivated us to evaluate its protein kinase inhibition profile and the resulting cellular consequences. The present work is thus directed toward analysis of the molecular effects in cancer cells of olomoucine II, a novel CDK inhibitor, with a focus on p53 activation.

Materials and methods

Compounds

R-roscovitine [(2-*R*)-2-(6-benzylamino-9-isopropyl-9*H*-purin-2-ylamino)-butan-1-ol)] and olomoucine II {2-{[2-((1-*R*)-1-hydroxymethyl-propylamino)-9-isopropyl-9*H*-purin-6-ylamino]-methyl}-phenol} were synthesized according to published procedures [7, 9]. For biological evaluation, compounds were made up as 100 mM stocks in dimethylsulfoxide (DMSO) and diluted prior to application in assay buffers or culture medium, respectively. The maximum concentration of DMSO in the assays never exceeded 0.1%.

Kinase inhibition

Kinase assays were performed using a 96-well plate format with recombinant CDK-cyclin complexes generated at Cyclacel, or with recombinant active ERK-2 or protein kinase Cα (Upstate Biotechnology). CDK1, CDK2, CDK4, CDK7, CDK9, SAPK2a (p38), and ERK-2 assays were performed using an assay buffer consisting of 25 mM β-glycerolphosphate, 20 mM MOPS, 5 mM EGTA, 1 mM DTT, and 1 mM $NaVO_3$ at pH 7.4, into which were added 2–4 μg of active enzyme with appropriate substrates [purified histone H1 for CDK1/cyclin B, CDK2/cyclin E, GST-pRb(773–928) for CDK2/cyclin A and CDK4/cyclin D1, biotinyl-Ahx-$(YSPTSPS)_4$ for CDK7/cyclin H and CDK9/cyclin T1, or myelin basic protein for SAPK2a (p38) and ERK-2). The reaction was initiated by addition of Mg/ATP mix (15 mM $MgCl_2$ and 100 μM ATP with 30–50 kBq per well of [γ-^{32}P]-ATP) and the mixtures were incubated for 10–45 min as required, at 30 °C. Reactions were stopped on ice, followed by filtration through p81 or GF/C filter plates (Whatman Polyfiltronics), except for CDK7 and CDK9, where, after stopping reactions on ice, 50 μg avidin was added to each well and incubation continued for 10 min prior to filtration. After washing three times with 75 mM aqueous orthophosphoric acid, plates were dried, scintillant (Microscint 40) added, and incorporated radioactivity measured in a scintillation counter (TopCount; Packard Instruments). Protein kinase C (PKC) and Protein kinase A (PKA) were assayed using commercial assay kits (Amersham Biotrak PKC and Upstate PKA assay kits). Data were analyzed using curve-fitting software (GraphPad Prism version 3.00 for Windows) to determine IC_{50} values (concentrations inhibiting kinase activity by 50%).

Crystallization and structure determination

Recombinant human CDK2 was produced and purified as previously described [22]. Briefly, CDK2 crystals were grown by vapor diffusion using the hanging-drop method. A solution of CDK2 (7–8 mg/ml in the final purification buffer) was mixed with the precipitant solution containing 15% PEG 6000 and 100 mM

Na-HEPES buffer (pH 7.5). Crystals were obtained after 3–5 days at 4 °C.

The olomoucine II/CDK2 complex was prepared by transferring a coverslip containing a drop of native CDK2 crystals over a well solution of 40% PEG 6000 and equilibrating at 4 °C for 24 h. A single crystal of CDK2 was transferred from this drop into a 2-µl drop of 40% PEG 6000, 100 mM Na-HEPES buffer (pH 7.5), 1 mM olomoucine II, and 5 mM DMSO, and placed over a well of the same solution. Crystals were left to soak for 7 days.

The crystal of about 0.05 mm in length was mounted in a 0.05- to 0.1-mm cryoloop (Hampton Research) and was flash frozen in liquid nitrogen. The soaking solution acted as a cryoprotectant. All diffraction data were collected at 100 K (Cryostream) at ESRF, Grenoble, on station ID14. Data processing was carried out using the programs MOSFLM and SCALA [23]. Initial structure solution was performed using the program MOLREP [24] using an available CDK2 structure (PDB code 1HCL). The program REFMAC [25] was used to perform refinement and ARP/WARP [26] was used to add water molecules. Refinement and model building were performed using the program O [27]. Atomic coordinates have been deposited in the Brookhaven Protein Data Bank under the accession code 2A0C.

Anticancer activity *in vitro*

The tumor cells (purchased from the American Type Culture Collection and the German Collection of Microorganisms and Cell Cultures) were grown in DMEM medium (Gibco BRL) supplemented with 10% (v/v) fetal bovine serum and L-glutamine (0.3 g/L) and were maintained at 37 °C in a humidified atmosphere with 5% CO_2. For anticancer cytotoxicity estimations, 10^4 cells were seeded into each well of a 96-well plate, allowed to stabilize for at least 4 h, and the test inhibitors were then added at various concentrations (ranging from 0.1 to 100 µM) in triplicate. Three days after addition of the inhibitors, calcein AM solution (Molecular Probes) was added. One hour later, fluorescence of cells was quantified using a Fluoroskan Ascent (Labsystems) reader and cytotoxic effective concentrations were calculated and expressed as IC_{50} values from dose-response curves. The p53 status of the cell lines was considered to be wild-type or mutant (including deletions) according to the relevant literature [28, 29].

p53-dependent transcriptional activity

To measure p53-dependent transcriptional activity, β-galactosidase activity was determined in the human melanoma cell line Arn8 which was established using stable transfection of the parental A375 cell line with a p53-responsive reporter construct pRGCΔfoslacZ [15] that allows qualitative as well as quantitative measurement of p53 transcriptional activity via β-galactosidase assay. After 24 h incubation with the inhibitors in a 96-well microtiter plate, the cells were fixed with 2% formaldehyde and 0.2% glutaraldehyde, washed with PBS, and developed in X-gal solution (0.2 mg/ml in PBS) overnight. Positive cells were scored under a light microscope. A 24-h incubation period was chosen, since by 6 h the level of p53 protein expression and its transcriptional activity had reached a steady state (data not shown).

Antibodies and immunoprecipitation

The monoclonal antibodies used in this study were: DO-1 antibody directed toward the epitope 20-SDLWKL-25 within the p53 N-terminal region [30, 31]; 118 antibody which recognizes the $p21^{WAF1}$ protein [32]; PC-10 antibody against PCNA [33]; 2A9 against Mdm2 [34], all produced and purified in-house. Anti-L11 (clone 3A4A7) was purchased from Zymed. The final antibody concentrations used for Western blotting were 1 µg/ml. For immunoprecipitation experiments, the cells were lysed in a buffer containing 150 mM NaCl, 50 mM Tris, pH 8.0, 5 mM EDTA, 1% NP40, 1 mM PMSF, supplemented with protease inhibitor cocktail, and incubated overnight at 4 °C with antibody, adsorbed onto protein G-Sepharose (Sigma), washed three times in lysis buffer, and analyzed by Western blotting.

SDS-polyacrylamide gel electrophoresis and Western blotting

For direct immunoblotting, total cellular protein lysates were prepared by harvesting cells in hot Laemmli electrophoresis sample buffer. Proteins were then separated by SDS-polyacrylamide gel electrophoresis on a 10% gel, and transferred onto a nitrocellulose membrane. Molecular-weight markers were run in parallel. The membrane was blocked in 5% low-fat milk and 0.1% Tween 20 in PBS for 2 h and probed overnight with the specific monoclonal antibodies described above. After washing three times in PBS plus 0.1% Tween 20, peroxidase-conjugated rabbit antimouse immunoglobulin antiserum diluted 1:2000 was used as the secondary antibody. To visualize peroxidase activity, ECL+ reagents were used according to the manufacturer's instructions.

Results

Kinase inhibition specificity

The potency of olomoucine II as an inhibitor was determined against a panel of purified human recombinant protein kinases, in the presence of a final ATP concentration of 100 µM as described elsewhere [35]. The data confirmed the specificity of olomoucine II for CDKs; apart from the main cell cycle-regulating kinase CDK2, it exerts specificity for CDK7 and CDK9, *i.e.* CDKs with important functions in the regulation of RNA transcription. Among them, CDK9 proved to be the most sensitive of all

Table 1. Kinase specificity of olomoucine II.

Kinase	Olomoucine II IC_{50} (μM)	*R*-roscovitine IC_{50} (μM)
CDK1/cyclin B	7.6±0.2	2.7±2-5
CDK2/cyclin E	0.1±0.01	0.1±0.1
CDK4/cyclin D1	19.8±0.2	14.2±4.3
CDK7/cyclin H	0.45±0.06	0.49±0.26
CDK9/cyclin T	0.06±0.02	0.74±0.09
Erk2	32±7	1.17±1.4
Abl	>100	>100
SAPK2a	>100	>20
PKCα	>100	>100
CaMKII	>100	n.a.
CKII	>100	n.a.
GSK3	>100	n.a.
PKA	>100	n.a.
PKB	>100	n.a.
PLK1	>100	n.a.
RSK	>100	n.a.

Recombinant kinases were assayed with 100 μM ATP as detailed in Materials and methods. Results are means (±SD) of three experiments. The values for *R*-roscovitine were taken from McClue et al. [35]. Abl, Abelson tyrosine kinase; CaMKII, calmodulin-dependent protein kinase II; CDK, cyclin-dependent kinase; CKII, casein kinase II; Erk2, extracellular signal-regulated kinase 2; GSK3, glycogen synthase kinase 3; PKA, protein kinase A; PKB, protein kinase B; PKCα, protein kinase Cα; PLK1, polo-like kinase 1; RSK, ribosomal S6 kinase; SAPK2a, stress-activated protein kinase 2a; n.a., data not available.

protein kinases tested (table 1). Most of the non-CDK kinases assayed were not inhibited, with the exception of Erk2, another target of the related purine CDK inhibitors roscovitine and purvalanols [8, 35]. Olomoucine II thus showed a better selectivity ratio for CDK9 than the structurally similar roscovitine, evident especially from the increase of inhibitory data for CDK1, CDK4 and Erk2, with 2.8-, 1.4-, and 30-fold higher IC_{50} values, respectively. CDK2 and CDK7 were affected approximately to the same extent by both olomoucine II and roscovitine. However, strong inhibition of the non-cell cycle-related CDK9 suggests that olomoucine II may significantly influence transcription in cells, which is controlled by RNA polymerase II, a natural substrate of CDK9.

Olomoucine II binding mode in CDK2

Since CDK9 has not been crystallized yet either alone or in a complex with a ligand, a co-crystal of CDK2 with the inhibitor was prepared and analyzed to understand the mechanism of anti-CDK action of olomoucine II in detail. As expected, the overall structure of CDK2 in the olomoucine II complex is very similar to those of the apo- and ATP-bound CDK2 structures [36]. The structure consists of two domains, the N-terminal domain (residues 1–83) composed predominately of β strands and the

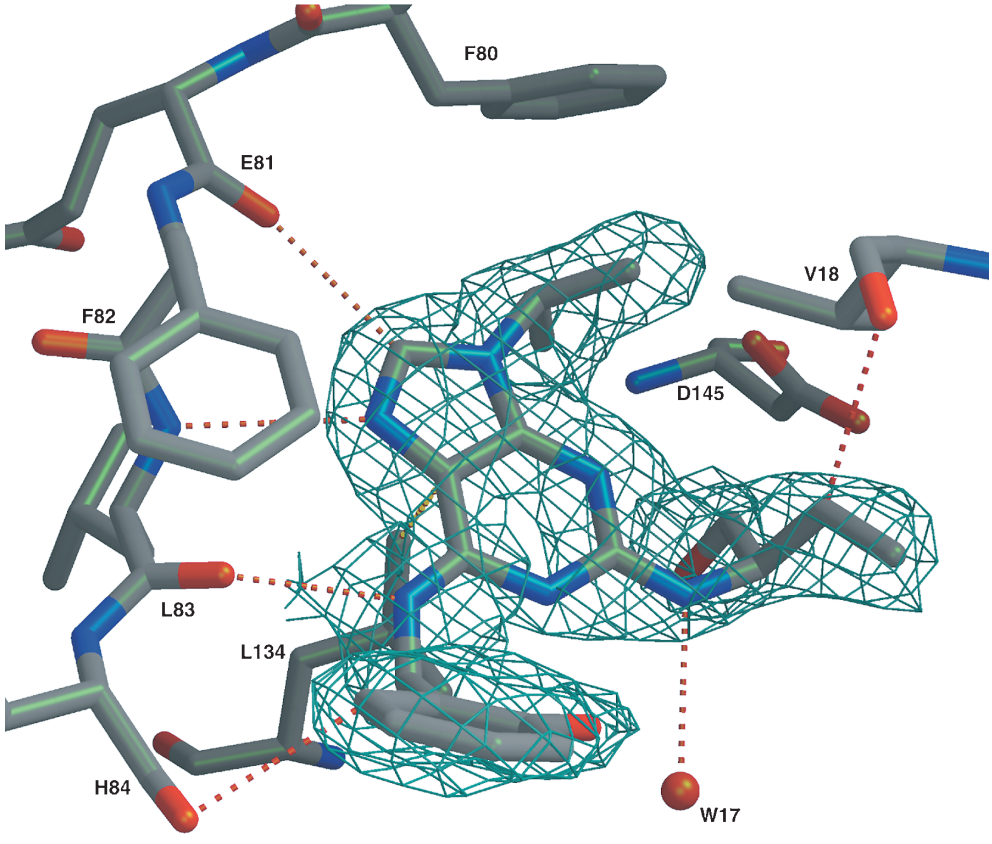

Figure 1. Refined electron density for olomoucine II localized within the active site of CDK2. 2|Fo|-|Fc| density is colored blue and is contoured at 1σ and shown around the ligand. All protein-ligand interactions less than 3.2 Å are indicated by a dashed red line.

C-terminal domain, which is mostly α helical. The final free R factor of the model is 24.4%.

Olomoucine II binds in the narrow cleft between the N- and C-terminal domains of CDK2. The electron density for the inhibitor is excellent with all its atoms being well defined in density and allowing the unambiguous positioning of the inhibitor in the binding cleft (fig. 1). The purine ring system of the ligand binds differently to the purine portion of ATP but in comparison with other homologous ligand structures (Protein Data Bank codes 1CKP and 1G5S [8, 37]), the purine ring is found to be in almost exactly the same position. The published binding modes and descriptions for both olomoucine and roscovitine [36, 38] also show that these compounds bind in a very similar mode to that of olomoucine II (coordinates for the two structures are not available). The purine ring is embedded between the side chains of Leu134 on one side (to which it makes a 3.18-Å interaction at C5 of the ligand) and Ile10 and Ala31 on the other side. As with other homologous ligand structures, olomoucine II forms two strong hydrogen bonds between the Leu83-N and Leu83-O backbone atoms using its N9 and N17 atoms as acceptor and donor, respectively. An additional conserved hydrogen bond is found between the Glu81-O and the CH8-hydrogen of the ligand. As with the 1G5S structure, the phenyl ring of the benzylamino group interacts with His84-O at the *ortho* position of the ring. This ring is in a similar orientation in both the olomoucine II and 1G5S structures. Additionally the *ortho* hydroxyl makes a good intramolecular hydrogen bond to N1 of the purine ring system (N...O=2.77 Å), stabilizing the orientation of the ring. Rotation of the ring by 180° results in the *ortho* hydroxyl being too close to the His84-O and no interaction between the *ortho* C..H and N1. Another protein-ligand interaction is found between C25 of the inhibitor and the CG1 of Val18. No other tight interactions are present for this section of the ligand to the protein. A further hydrogen bond is found from N13 to a well-defined water molecule (W17). This water molecule makes additional bonds with the side chain of Asp86 and Gln131. A longer (3.4 Å) interaction is made between this water and the *ortho* hydroxyl of the inhibitor phenol ring. The W17 water is not present in either 1CKP or 1G5S, although this may be a consequence of the lower resolution of the 1G5S structure (2.61 Å). Interestingly, the purvalanol structure contains a molecule of ethanediol in the active site. One of the oxygens of the ethanediol is in a position similar to that of the hydroxyl of the N13 substituent of olomoucine II. The ethanediol forms a hydrogen bond to the backbone O of Gln131. This distance is increased to 3.4 Å in the olomoucine II structure. Also apparent in the purvalanol structure is that the presence of ethanediol produces disordering of Asn132 into two distinct positions; in one of these, the Gln131-binding O of ethanediol is able to form a strong hydrogen bond to the side chain of Asn132.

Table 2. *In vitro* antiproliferative activity of CDK inhibitors on human cancer cell lines of different origin and p53 status.

Cell line	Tissue origin (p53 status)	Olomoucine II IC_{50} (μM)	*R*-roscovitine IC_{50} (μM)
HOS	bone (mut)	9.3±2.4	24.3±0.2
T98G	brain (mut)	9.2±0.9	29.0±2.2
HBL100	breast (wt)	10.5±3.0	13.9±3.4
BT474	breast (mut)	13.6±0.3	30.5±3.4
MCF-7	breast (wt)	5.0±3.0	12.3±1.1
HT29	colon (mut)	10.8±0.3	25.6±1.9
CCRF-CEM	blood (mut)	5.3±0.8	16.3±1.7
BV173	blood (wt)	2.7±0.6	15.8±2.3
HL60	blood (mut)	16.3±0.1	33.2±8.8
K562	blood (mut)	11.5±3.1	45.5±2.7
Hs913T	lung (mut)	10.3±1.4	24.5±4.7
A549	lung (wt)	8.7±0.7	25.0±4.1
A431	skin (mut)	10.2±0.5	30.0±1.9
SVK14	skin (wt)	9.3±2.0	29.9±6.5
G361	skin (wt)	7.8±0.4	22.4±0.2
SKUT-1	uterus (mut)	4.9±0.2	22.0±0.7
HeLa	uterus (wt)	7.7±0.3	22.3±2.1
Mean	(wt)	7.4	20.2
Mean	(mut)	10.1	28.1

The number of viable cells after 72 h treatment of cell cultures was quantified with the calcein method and IC_{50} values were calculated from dose-response curves. Results are means (±SD) of at least three experiments. wt, wild type; mut, mutant

This disordering is not present in the ligand structure and the Asn132 side chain points away from the active site. The movement of this hydroxyl toward either Gln131 or Asn132 is probably restricted by the presence of the ethanyl group moving too close to Val18 and stopping this hydrogen bond pattern forming. The enantiomeric form of the compound should change the binding pattern in this region.

Also interesting to note is that the orientation of Lys33 (which is very well defined in the structure) is found in the *trans* configuration suggested by Wu et al. [22] to play a role in the disordering of the T loop of CDK2. In the structure discussed here, the T loop is also disordered as it is in the purvalanol B, olomoucine, and roscovitine complexes [8, 36, 38].

Anticancer activity *in vitro*

Our previous comparison of olomoucine II and roscovitine cytotoxicities on five different cell lines already suggested increased cellular activity of the novel compound [9]. The antiproliferative activity of olomoucine II was therefore verified on a panel of 17 human tumor cell lines and compared with that of roscovitine using a fluorescent indicator of cell viability and intact membranes calcein [39]. After 72-h incubation of tumor cells with olomoucine II, we found this compound to be more than two-fold more potent than roscovitine. These data demonstrated a wide range of effectivity against cell lines derived from various human tumor tissues, with slightly increased

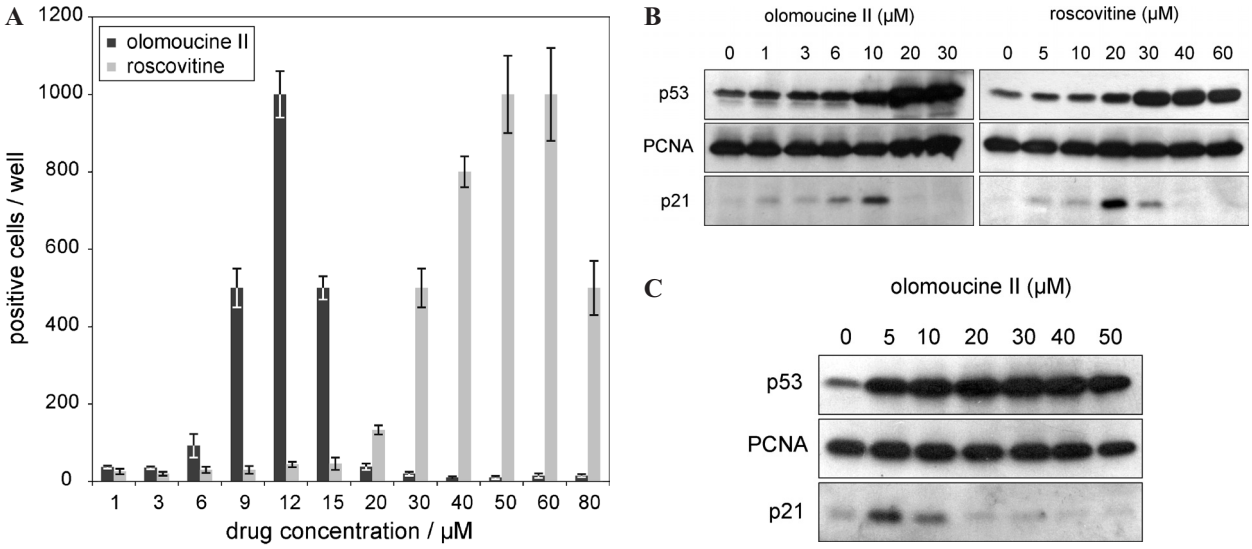

Figure 2. Dose-dependent effect of olomoucine II and roscovitine on p53-dependent transcription. (*A*) Arn8 cells stably transfected with a p53-responsive β-galactosidase reporter construct were treated with different CDK inhibitors for 24 h and positive cells were counted under a light microscope for each concentration in triplicate. (*B*) Induction of p53 and p21^{WAF1} proteins in Arn8 cells treated with the indicated concentrations of CDK inhibitors. (*C*) Induction of p53 and p21^{WAF1} proteins in MCF-7 after olomoucine II treatment. The cells were harvested, the proteins were separated on a 10% SDS-PAGE gel and analyzed on Western blots with specific antibodies as described in Materials and methods.

potency against cells harboring a wild-type p53 gene (table 2). Of the 17 cell lines used, 10 were considered to bear mutant p53 with average IC_{50} values estimated to be approximately 1.4-fold higher than for cells with wild-type p53 (Student's *t*-test, $p = 0.096$). Such a tendency has already been described for the related compound roscovitine [35]. On the other hand, leukemia CCRF-CEM and sarcoma SKUT-1 cell lines with inactive p53 showed markedly higher sensitivity to olomoucine II over the average IC_{50}. The difference between average cell cytotoxicity of roscovitine measured in our laboratory and the value published earlier (IC_{50}=15.2 μM [35]) is due to a different assay method and a different cell line panel. However, the results support the correlation between CDK inhibitory activity of 2,6,9-trisubstituted purines and their *in vitro* anticancer activity that we described earlier [40].

Olomoucine II induces p53-dependent transcription

With respect to the preferential affinity of olomoucine II for CDK9, we attempted to verify this influence on transcription in a cell-based assay in the human melanoma cell line Arn8 expressing β-galactosidase under the control of a p53-responsive promoter. Accumulation of wild-type p53 in the treated cell line led to activation of the responsive promoter and subsequent expression of β-galactosidase. After 24 h, Arn8 cells incubated with medium containing increasing doses of olomoucine II were fixed and monitored for galactosidase activity using the X-gal substrate. A substantial (50-fold) increase of the number of positive cells appeared at compound concentrations ranging from 9 to 15 μM. Higher amounts of olomoucine II led to inhibition of p53 activity back to basal level. In a control experiment run in parallel, roscovitine proved to be active from 30 μM (fig. 2A).

The reporter-based assay was complemented with Western blotting analysis of p53 and p21^{WAF1} proteins in ARN8 and MCF7 cells. Similarly, an enhancement of p53 signal was observed in olomoucine II-treated cells in a dose-dependent manner, beginning at concentrations as low as 5 μM. Together with p53, its downstream target gene product p21^{WAF1} was also co-induced and detected in both cell lines (fig. 2B, C). However, higher doses of olomoucine II (above 10 μM in Arn8 and 5 μM in MCF-7) again suppressed the transcriptional activity of p53, so that p21^{WAF1} was no longer detectable in cells. Roscovitine, already known to have similar effects, was active at higher concentrations, with p21^{WAF1} peaking at around 20 μM in Arn8 cells (fig. 2B).

CDK inhibitors increase L11 complexing of Mdm2

Our data supported the idea that roscovitine and olomoucine II can induce transcription stress by inhibition of CDKs. This stress is responsible for nucleolus disintegration [13, 14, 20]. We analyzed the role of transcription stress (mediated by low concentrations of olomoucine II and roscovitine) in the activation of p53 protein. Since L11 is a nucleolar and ribosomal protein that binds to and inactivates Mdm2 as ribosomal stress occurs [41], we examined the influence of CDK inhibitors on its distribution. When Mdm2 was immunoprecipitated from Arn8 and MCF-7 cells treated with CDK inhibitors, the L11 protein

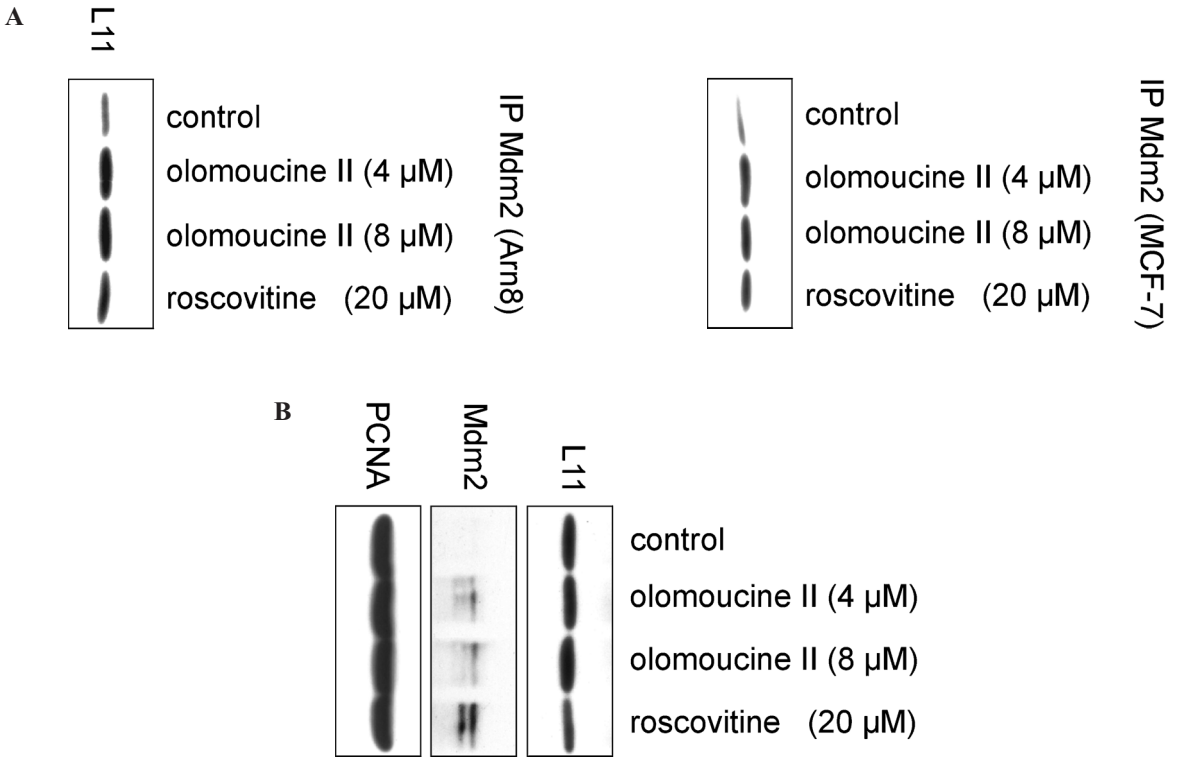

Figure 3. L11 binding to Mdm2 in Arn8 and MCF-7 cells treated with the indicated CDK inhibitors. (*A*) Cells were incubated with olomoucine II and roscovitine for 24 h, lysed and immunoprecipitated with the anti-Mdm2 antibody followed by Western blotting probed with anti-L11 antibody. (*B*) Direct Western blot analysis of the Arn8 cells treated with olomoucine II and roscovitine for 24 h did not reveal any obvious differences in L11 level, but showed an increase in Mdm2. Sample loading order as in *A*.

was also found to be bound to Mdm2 by Western blotting using a specific anti-L11 antibody (fig. 3A), in contrast to control cells that contained insignificant amounts of the L11-Mdm2 complex. As expected, cell lysates analyzed for their L11 level did not show any obvious differences, but confirmed activation of Mdm2 by both CDK inhibitors (fig. 3B).

Discussion

The relatively small structural variation between roscovitine and olomoucine II, which differs from roscovitine only by the presence of an additional *ortho*-hydroxyl group in the benzyl function, was found to significantly change the protein kinase inhibition specificity toward CDK9. A crystal structure of olomoucine II complexed with CDK2 was prepared and analyzed; however, the preference of the inhibitor converges on CDK9, which is involved in transcription and thus different molecular effects could be expected in cells, presumably similar to those of another CDK inhibitor with CDK9 specificity, *i.e.* flavopiridol [17, 19]. Since a method for CDK9 crystallization has not yet been described, a co-crystal of olomoucine II with CDK2 was analyzed to gain better insight into the inhibition specificity. The olomoucine II molecule occupies almost exactly the same position in CDK2 compared with other homologous ligand complex structures such as those of purvalanol B, olomoucine, H717, and roscovitine [8, 36–38]. In the olomoucine II structure, the phenolic hydroxyl forms an intramolecular hydrogen bond to N1 of the purine ring system and this stabilizes the orientation of the ring. Moreover, a CH group of the phenyl ring interacts with the His84 carbonyl oxygen and this may contribute to increased ligand affinity to CDK2 (and possibly also to CDK9). According to the *in silico* model of CDK9 with bound flavopiridol, strong electrostatic interactions between Glu92-Lys20 and Glu92-Lys29, involving residues not present in CDK2, render the binding pocket tighter and increase the contact area between protein and inhibitor [19]. As a consequence of these interactions, the phenyl side chain of Phe90 is also pushed deeper into the ATP-binding pocket, closing the pocket and further increasing the contact area of CDK9 not only for flavopiridol but probably also for purines including olomoucine II [19].

The increased antiproliferative activity of olomoucine II over roscovitine that had been measured previously [9] was confirmed here in a panel of 17 human tumor cell lines of different tissue origin: the inhibitor proved to be effective on all cell lines. Efficacy on cells harboring wild-type p53 was approximately 1.4-fold higher than on

those with mutant p53, which is very similar to roscovitine, calculated to be 1.5 [35]. Similarly, other CDK inhibitors (flavopiridol and kenpaullone) also exert higher activity on cells with active p53 according to a publicly available database of *in vitro* antitumor cell line-screening results of the National Cancer Institute [28, 29]. On the other hand, the fact that the difference in average sensitivity between p53 normal and mutated cells does not exceed one order of magnitude and that CDK inhibitors display antiproliferative activity on all cells irrespective of p53 status suggest that p53 plays only a partial role in the cellular response. Moreover, although the antiproliferative activities of CDK inhibitors have been generally thought to correlate with their inhibition of CDK1, CDK2, and CDK4, leading to dephosphorylation of substrates relevant to these CDKs, and blockage of the cell cycle, recent reports suggest that other non-cell cycle-related targets should also be taken into account. This aspect has recently been revised in the case of flavopiridol which also inhibits other homologous kinases, CDK7–9, involved in the initiation and elongation phases of RNA transcription [8, 19, 42]. Nevertheless, purine CDK inhibitors affect RNA synthesis in cells as well and the mechanism involves inhibition of the phosphorylation of the CTD of RNA polymerase II [8, 16, 18].

Another phenomenon usually accompanying the cellular effects of CDK inhibitors is accumulation of p53 protein and subsequent induction of the downstream $p21^{WAF1}$ gene in cells with wild-type p53 [13, 15, 17]. The latest reports provide evidence that the accumulation of p53 followed by *trans*-activation of Mdm2 and $p21^{WAF1}$ results from direct inhibition of transcription caused by pharmacological CDK inhibition [17, 18]. Thus, with respect to its specificity, the induction of p53-dependent transcription activity by low doses of olomoucine II can also be directly ascribed to inhibition of CDK9, leading to initial down-regulation of the short half-life negative p53 regulator Mdm2 and stabilization of p53 protein levels. Virtually identical results have been recently demonstrated in HCT116 cells treated with flavopiridol [17]. Conversely, higher concentrations of olomoucine II (and also roscovitine and flavopiridol [16, 17]) decreased transcription in cells in general, leading to a drop in p53 activity, as seen in a cell-based assay and also on $p21^{WAF1}$ levels on Western blots. As concluded from the relevant experiments with flavopiridol, the transcription inhibition is transient at low drug concentrations and the transcription is restored slowly over time [17].

Except for inhibition of transcription by anti-CDK agents that leads to a direct drop in Mdm2, we suggest an alternative explanation for the p53-activating pathway. Ribosomal stress is known to trigger release of several proteins from ribosomes. According to our observation and to other reports [13, 14, 20, 21], olomoucine II and roscovitine (data not shown) are also able to disintegrate nucleoli. One of the proteins released from the nucleoli is L11 which then interacts with Mdm2 and blocks its ubiquitinating activity against p53 [41, 43]. Under normal conditions, L11 is localized to the nucleolus where it participates in ribosomal biogenesis and after transcription perturbation or disruption of nucleoli it translocates to the nucleoplasm where it stabilizes p53 [41, 43, 44]. Stabilized p53 can thereby *trans*-activate its subordinated genes; one results is that Mdm2 complexed with L11 is no longer able to ubiquitinate p53 [43]. Therefore, nucleolar disruption may inhibit p53 ubiquitination which results in its nuclear accumulation [44, 45].

The exact roles of the studied compounds in nucleolar destruction remain to be explored. However, speculation arises as to the possible inhibition of RNA polymerase III which also leads to breakdown of nucleolar structure and stabilization of p53 [44, 45]. Such a mechanism could utilize repression of TFIIIB by pRb, a substrate of CDK2 and CDK4, that in hypophosphorylated form suppresses transcription driven by RNA polymerase III [46]. In summary, the observed effects of CDK inhibitors are likely to imitate DNA damage through multiple transcription disturbances, sensed by rate of transcription, serving the cell as a lesion dosimeter of genome integrity and inducing cell destruction [45].

Acknowledgements. This work was supported by grants GA CR 204/03/D231, IGA MZ CR NC6652-3 (both to V. K.) and NC7131-3 (to P. M. and B. V.), and MSM 6198959216 (to M. S. and L. H.). The authors thank the protein biochemistry and assay development and screening group members at Cyclacel for their contribution to the work presented here.

1 Sherr C. J. (1996) Cancer cell cycles. Science **274:** 1672–1677
2 Morgan D. O. (1995) Principles of CDK regulation. Nature **374:** 131–134
3 Pinhero R., Liaw P., Bertens K. and Yankulov K. (2004) Three cyclin-dependent kinases preferentially phosphorylate different parts of the C-terminal domain of the large subunit of RNA polymerase II. Eur. J. Biochem. **5:** 1004–1014
4 Meijer L. and Raymond E. (2003) Roscovitine and other purines as kinase inhibitors: from starfish oocytes to clinical trials. Acc. Chem. Res. **36:** 417–425
5 Fischer P. M., Endicott J. and Meijer L. (2003) Cyclin-dependent kinase inhibitors. Prog. Cell Cycle Res. **5:** 235–248
6 Vesely J., Havlicek L., Strnad M., Blow J. J., Donella-Deana A., Pinna L. et al. (1994) Inhibition of cyclin-dependent kinases by purine analogues. Eur. J. Biochem. **224:** 771–786
7 Havlicek L., Hanus J., Vesely J., Leclerc S., Meijer L., Shaw G. et al. (1997) Cytokinin-derived cyclin-dependent kinase inhibitors: synthesis and cdc2 inhibitory activity of olomoucine and related compounds. J. Med. Chem. **40:** 408–412
8 Gray N. S., Wodicka L., Thunnissen A. M., Norman T. C., Kwon S., Espinoza F. H. et al. (1998) Exploiting chemical libraries, structure, and genomics in the search for kinase inhibitors. Science **281:** 533–538
9 Krystof V., Lenobel R., Havlicek L., Kuzma M. and Strnad M. (2002) Synthesis and biological activity of olomoucine II. Bioorg. Med. Chem. Lett. **12:** 3283–3286
10 Fischer P. M. and Gianella-Borradori A. (2003) CDK inhibitors in clinical development for the treatment of cancer. Expert Opin. Invest. Drugs **12:** 955–970

11 Fischer P. M. and Gianella-Borradori A. (in press) Recent progress in the discovery and development of CDK inhibitors. Expert Opin. Invest. Drugs **14:** 457–477
12 Sielecki T. M., Boylan J. F., Benfield P. A. and Trainor G. L. (2000) Cyclin-dependent kinase inhibitors: useful targets in cell cycle regulation. J. Med. Chem. **43:** 1–18
13 David-Pfeuty T. (1999) Potent inhibitors of cyclin-dependent kinase 2 induce nuclear accumulation of wild-type p53 and nucleolar fragmentation in human untransformed and tumor-derived cells. Oncogene **18:** 7409–7422
14 Wojciechowski J., Horky M., Gueorguieva M. and Wesierska-Gadek J. (2003) Rapid onset of nucleolar disintegration preceding cell cycle arrest in roscovitine-induced apoptosis of human MCF-7 breast cancer cells. Int. J. Cancer **106:** 486–495
15 Kotala V., Uldrijan S., Horky M., Trbusek M., Strnad M. and Vojtesek B. (2001) Potent induction of wild-type p53-dependent transcription in tumour cells by a synthetic inhibitor of cyclin-dependent kinases. Cell. Mol. Life Sci. **58:** 1333–1339
16 Ljungman M. and Paulsen M. T. (2001) The cyclin-dependent kinase inhibitor roscovitine inhibits RNA synthesis and triggers nuclear accumulation of p53 that is unmodified at Ser15 and Lys382. Mol. Pharmacol. **60:** 785–789
17 Demidenko Z. N. and Blagosklonny M. V. (2004) Flavopiridol induces p53 via initial inhibition of Mdm2 and p21 and, independently of p53, sensitizes apoptosis-reluctant cells to tumor necrosis factor. Cancer Res. **64:** 3653–3660
18 Whittaker S. R., Walton M. I., Garrett M. D. and Workman P. (2004) The cyclin-dependent kinase inhibitor CYC202 (R-roscovitine) inhibits retinoblastoma protein phosphorylation, causes loss of cyclin D1, and activates the mitogen-activated protein kinase pathway. Cancer Res. **64:** 262–272
19 Azevedo W. F de. Jr, Canduri F. and Silveira N. J. da (2002) Structural basis for inhibition of cyclin-dependent kinase 9 by flavopiridol. Biochem. Biophys. Res. Commun. **293:** 566–571
20 Schlosser I., Holzel M., Murnseer M., Burtscher H., Weidle U. H. and Eick D. (2003) A role for c-Myc in the regulation of ribosomal RNA processing. Nucleic Acids Res. **31:** 6148–6156
21 Sirri V., Hernandez-Verdun D. and Roussel P. (2002) Cyclin-dependent kinases govern formation and maintenance of the nucleolus. J. Cell Biol. **156:** 969–981
22 Wu S. Y., McNae I., Kontopidis G., McClue S. J., McInnes C., Stewart K. J. et al. (2003) Discovery of a novel family of CDK inhibitors with the program LIDAEUS: structural basis for ligand-induced disordering of the activation loop. Structure **11:** 399–410
23 Leslie A. G. W. (1992) Recent changes to the MOSFLM package for processing film and image plate data. Joint CCP4 + ESF-EAMCB Newsletter on Protein Crystallography **26**
24 Vagin A. and Teplyakov A. (1997) MOLREP: an automated program for molecular replacement. J. Appl. Crystallogr. **30:** 1022–1025
25 Murshudov G. N., Vagin A. A. and Dodson E. J. (1997) Refinement of macromolecular structures by the maximum-likelihood method. Acta Cryst. D **53:** 240–255
26 Lamzin V. S. and Wilson K. S. (1997) Automated refinement for protein crystallography. Methods Enzymol. **277:** 269–305
27 Jones T. A., Zou J. Y., Cowan S. W. and Kjeldgaard M. (1991) Improved methods for building protein models in electron density maps and the location of errors in these models. Acta Crystallogr A Found. Crystallogr. A **47:** 110–119
28 O'Connor P. M., Jackman J., Bae I., Myers T. G., Fan S., Mutoh M. et al. (1997) Characterization of the p53 tumor suppressor pathway in cell lines of the National Cancer Institute anticancer drug screen and correlations with the growth-inhibitory potency of 123 anticancer agents. Cancer Res. **57:** 4285–4300
29 Olivier M., Eeles R., Hollstein M., Khan M.A., Harris C.C. and Hainaut P. (2002) The IARC TP53 Database: new online mutation analysis and recommendations to users. Hum. Mutat. **19:** 607–614
30 Vojtesek B., Bartek J., Midgley C. A. and Lane D. P. (1992) An immunochemical analysis of the human nuclear phosphoprotein p53: new monoclonal antibodies and epitope mapping using recombinant p53. J. Immunol. Methods **151:** 237–244
31 Stephen C. W., Helminen P. and Lane D. P. (1995) Characterisation of epitopes on human p53 using phage-displayed peptide libraries: insights into antibody-peptide interactions. J. Mol. Biol. **248:** 58–78
32 Fredersdorf S., Milne A. W., Hall P. A. and Lu X. (1996) Characterization of a panel of novel anti-p21Waf1/Cip1 monoclonal antibodies and immunochemical analysis of p21Waf1/Cip1 expression in normal human tissues. Am. J. Pathol. **148:** 825–835
33 Waseem N. H. and Lane D. P. (1990) Monoclonal antibody analysis of the proliferating cell nuclear antigen (PCNA): structural conservation and the detection of a nucleolar form. J. Cell Sci. **96:** 121–129
34 Chen J., Marechal V. and Levine A. J. (1993) Mapping of the p53 and mdm-2 interaction domains. Mol. Cell. Biol. **13:** 4107–4114
35 McClue S. J., Blake D., Clarke R., Cowan A., Cummings L., Fischer P. M. et al. (2002) In vitro and in vivo antitumor properties of the cyclin dependent kinase inhibitor CYC202 (R-roscovitine). Int. J. Cancer **102:** 463–468
36 Schulze-Gahmen U., Brandsen J., Jones H. D., Morgan D. O., Meijer L., Vesely J. et al. (1995) Multiple modes of ligand recognition: crystal structures of cyclin-dependent protein kinase 2 in complex with ATP and two inhibitors, olomoucine and isopentenyladenine. Proteins **22:** 378–391
37 Dreyer M. K., Borcherding D. R., Dumont J. A., Peet N. P., Tsay J. T., Wright P. S. et al. (2000) Crystal structure of human cyclin-dependent kinase 2 in complex with the adenine-derived inhibitor H717. J. Med. Chem. **44:** 524–530
38 De Azevedo W. F., Leclerc S., Meijer L., Havlicek L., Strnad M. and Kim S. H. (1997) Inhibition of cyclin-dependent kinases by purine analogues: crystal structure of human cdk2 complexed with roscovitine. Eur. J. Biochem. **243:** 518–526
39 Lichtenfels R., Biddison W. E., Schulz H., Vogt A. B. and Martin R. (1994) CARE-LASS (calcein-release-assay), an improved fluorescence-based test system to measure cytotoxic T lymphocyte activity. J. Immunol. Methods **172:** 227–239
40 Vermeulen K., Strnad M., Krystof V., Havlicek L., Van der Aa A., Lenjou M. et al. (2002) Antiproliferative effect of plant cytokinin analogues with an inhibitory activity on cyclin-dependent kinases. Leukemia **16:** 299–305
41 Zhang Y., Wolf G. W., Bhat K., Jin A., Allio T., Burkhart W. A. et al. (2003) Ribosomal protein L11 negatively regulates oncoprotein MDM2 and mediates a p53-dependent ribosomal-stress checkpoint pathway. Mol. Cell. Biol. **23:** 8902–8912
42 Chao S. H., Fujinaga K., Marion J. E., Taube R., Sausville E. A., Senderowicz A.M. et al. (2000) Flavopiridol inhibits P-TEFb and blocks HIV-1 replication J. Biol. Chem. **275:** 28345–28348
43 Bhat K., Itahana K., Jin A. and Zhang Y. (2004) Essential role of ribosomal protein L11 in mediating growth inhibition-induced p53 activation. EMBO J. **23:** 2402–2412
44 Rubi C. P. and Milner J. (2003) Disruption of the nucleolus mediates stabilization of p53 in response to DNA damage and other stresses. EMBO J. **22:** 6068–6077
45 Ljungman M. and Lane D. P. (2004) Transcription – guarding the genome by sensing DNA damage. Nat. Rev. Cancer **4:** 727–737
46 White R. J. (2004) RNA polymerase II transcription and cancer. Oncogene **23:** 3208–3216